

Absence of Intrinsic Ferromagnetic Interactions of Isolated and Paired Co Dopant Atoms in $\text{Zn}_{1-x}\text{Co}_x\text{O}$ with High Structural Perfection

A. Ney,^{1,*} K. Ollefs,¹ S. Ye,¹ T. Kammermeier,¹ V. Ney,¹ T. C. Kaspar,² S. A. Chambers,² F. Wilhelm,³ and A. Rogalev³

¹*Fachbereich Physik and Center for Nanointegration Duisburg-Essen (CeNIDE), Universität Duisburg-Essen, Lotharstrasse 1, D-47057 Duisburg, Germany*

²*Fundamental and Computational Sciences Directorate, Pacific Northwest National Laboratory, Richland, Washington 99352, USA*

³*European Synchrotron Radiation Facility (ESRF), 6 Rue Jules Horowitz, BP 220, 38043 Grenoble Cedex, France*

(Received 29 October 2007; published 15 April 2008)

We report element specific structural and magnetic investigations on $\text{Zn}_{1-x}\text{Co}_x\text{O}$ epitaxial films using synchrotron radiation. Co dopants exclusively occupy Zn sites as revealed by x-ray linear dichroism having an unprecedented degree of structural perfection. Comparative magnetic field dependent measurements by x-ray magnetic circular dichroism and conventional magnetometry consistently show purely paramagnetic behavior for isolated Co dopant atoms with a magnetic moment of $4.8\mu_B$. However, the total magnetization is reduced by $\sim 30\%$, demonstrating that Co-O-Co pairs are antiferromagnetically coupled. We find no sign of intrinsic ferromagnetic interactions for isolated or paired Co dopant atoms in Co:ZnO films.

DOI: [10.1103/PhysRevLett.100.157201](https://doi.org/10.1103/PhysRevLett.100.157201)

PACS numbers: 75.50.Pp, 75.25.+z, 75.70.-i

Dilute magnetic semiconductors (DMS) are envisioned as sources of spin polarized carriers for future semiconductor devices which would simultaneously utilize the spin and charge of the carriers. Practical device technology requires that the magnetic order is present at and above room temperature. $\text{Zn}_{1-x}\text{Co}_x\text{O}$ (Co:ZnO) has been thought to be a promising candidate *n*-type DMS, and has been widely studied. Although Co:ZnO and other candidate DMS materials have been intensively investigated, their respective magnetic behaviors remain controversial from both experimental and theoretical points of view. Claims of room-temperature ferromagnetism, or the absence of same, have been made by both experimentalists and theorists, see Ref. [1] for a recent discussion. Room-temperature magnetic order in Co:ZnO films can be reversibly activated and deactivated by cycles of Zn diffusion and air annealing, suggesting that charge carriers associated with interstitial Zn (a shallow donor) play a crucial role in the magnetic behavior [2]. Nevertheless, the possibility that metallic Co nanoclusters play an important role in accounting for the observed magnetic order cannot be dismissed, as shown recently by careful x-ray diffraction analysis [3]. Detailed studies using synchrotron radiation have been performed to rule out phase separation based on the shape of the absorption spectrum at the Co *K* edge for Co:ZnO [2]. The absence of Co-sublattice ferromagnetic order was reported for magnetron-sputtered 10% Co:ZnO by means of x-ray magnetic circular dichroism (XMCD) measurements. However, superconducting quantum interference device (SQUID) magnetometry showed long-range magnetic order at room temperature so that the results remain inconsistent [4]. Measurements of the x-ray linear dichroism (XLD) for Mn:GaN [5] and Gd:GaN [6] ruled out phase separation and antisite disorder but XMCD failed to prove ferromagnetism at elevated temperatures. For Cr:TiO₂ it

was shown before that in samples with high structural perfection ferromagnetism is negligible [7]. Therefore, a combined structural and magnetic characterization is a reliable way of proving or disproving intrinsic ferromagnetism in DMS.

Here we present element specific investigations of Co:ZnO at the Zn and Co *K* edges, respectively, measuring the XLD as well as the XMCD. We show that virtually all ($\sim 95\%$) Co dopants are incorporated on cation lattice sites. The $M(H)$ curves measured by XMCD at the Co *K* edge and SQUID indicate pure paramagnetic behavior. We infer a magnetic moment of $4.8\mu_B/\text{Co}$ atom. A quantitative analysis of the size of the magnetization versus the product of the magnetic moment and the number of Co atoms indicates that Co-O-Co pairs are coupled antiferromagnetically. No signatures of intrinsic ferromagnetic interactions for isolated and paired Co dopant atoms are found.

$\text{Co}_{0.1}\text{Zn}_{0.9}\text{O}(0001)$ epitaxial films were grown on epitaxially *c*-sapphire substrates using pulsed laser deposition at a substrate temperature of 550 °C and an O₂ pressure of 10 mTorr. The laser repetition rate and power level were 1 Hz and (314 ± 5) mJ/pulse, respectively, yielding 2.4 J/cm² incident on the target, and the growth rate was 0.25 Å/sec. The film thickness was 105 nm as measured by x-ray reflectivity and the concentration *x* of Co atoms was 10.8% as measured by proton-induced x-ray emission. X-ray diffraction indicates high structural perfection with a full-width at half maximum (FWHM) of 0.38° in ω -rocking curves of the (0002) reflection of ZnO which itself has a FWHM of less than 0.15° in the $\omega - 2\theta$ scan. The x-ray absorption near edge spectra (XANES) were taken at the ESRF ID 12 beam line in total fluorescence yield [8] and all absorption spectra were normalized with respect to the edge jump. For the XLD measurements a

quarter wave plate was used to flip the linear polarization of the synchrotron light from vertical to horizontal as described in greater detail elsewhere [5,8]; the angle of incidence was 10° with respect to the sample surface. The XMCD measurements were taken as the direct difference of XANES spectra recorded with right and left circular polarized light under grazing incidence (10°). The XMCD spectra were recorded in an external magnetic field of ± 6 T provided by a superconducting magnet in order to minimize artifacts. The XLD and XANES spectra were simulated using the FDMNES code [9] using the multiple scattering formalism within the muffin-tin approximation. Additional in-plane magnetic measurements were performed using a commercial SQUID magnetometer which was calibrated with both a Ni and a Pd reference sample prior to the measurement.

Figure 1(a) shows the experimental XANES spectra (full symbols) recorded at the Zn *K* edge at room temperature with the electric field vector of the x rays perpendicular (squares) and parallel (circles) to the *c* axis. The associated XLD signal, obtained by taking the difference of the XANES spectra for the two polarizations, is given in Fig. 1(b). Because of the uniaxial crystal symmetry of the wurtzite lattice, the final states are split by the crystal field. Hence, the XLD is purely a result of the structure. Figure 1 also shows the simulated spectra (open symbols). These were calculated using the bulk lattice constants ($a = 3.2459$ Å and $c = 5.2069$ Å), a dimensionless u parameter of 0.382 for wurtzite ZnO [10], a core hole lifetime (FWHM) of 1.67 eV for Zn [11], and an arctangentlike energy-dependent broadening. The same broadening parameters were used for simulating the Co spectra. Our findings are distinct from a previous study [4] in two regards: (i) the authors in Ref. [4] report a maximum XLD signal at the Zn *K* edge of $(60 \pm 3)\%$ of the edge jump compared with $(70 \pm 1)\%$ for our sample indicating less perfect local crystallographic order and (ii) the radius of the cluster used for the simulations was increased from 6 to 8.5 Å to improve the accuracy of the calculation and to better reproduce the details of the XLD spectrum. The $(\text{Zn}_{23}\text{Co})\text{O}_{24}$ supercell we used yields identical results for the Zn XLD as a pure ZnO cell. The experimental and simulated spectra were normalized at the same energies, and the good quantitative agreement demonstrates that each Zn atom is locally surrounded by the bulk ZnO wurtzite structure. The discrepancy between experiment and simulation around 9680 eV originates from the muffin-tin approximation [9] and is also visible in other simulations [4–6].

Figure 2(a) shows the experimental and calculated XANES spectra at the Co *K* edge with a maximum signal of $(39 \pm 1)\%$ of the edge jump. In comparison, the previously studied Co:ZnO samples fabricated by sputtering [4] derived a maximum XLD signal of only $(32 \pm 2)\%$. In turn this means that in the previous studies at least 10% of the Co dopants are *not* in a local wurtzite environment which could—in principle—account for the observed re-

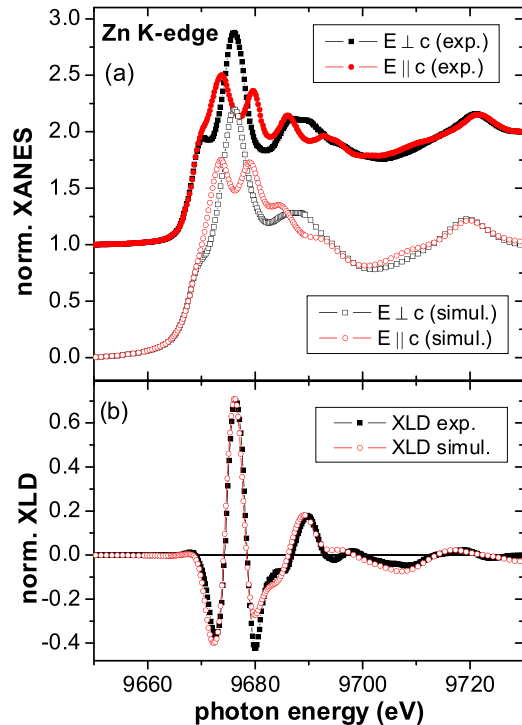


FIG. 1 (color online). (a) Measured and calculated XANES spectra at the Zn *K* edge of ZnO for two perpendicular orientations of the linear polarization of the light. The measurements were taken at 300 K under 10° grazing incidence. (b) Respective calculated and measured XLD signatures.

sidual hysteresis of $\sim 0.25 \mu_B/\text{Co atom}$ at 300 K in [4]. For the simulations a core hole lifetime of 1.33 eV was used for Co [11]. Simulations were also carried out for Co on O sites (antisites), for Co-Co pairs, and Co-O-Co pairs. Co antisites and Co-Co pairs have a significantly different XLD signature marked by different peak amplitudes, positions, and signs (not shown), whereas Co on random interstitial sites would only reduce the amplitude of the normalized XLD signal. The simulation of Co-O-Co pairs slightly reduces the peak around 7740 eV (arrow in Fig. 2), where the agreement between experiment and simulation is not as good; the disagreement around 7730 eV again originates from the muffin-tin approximation. Because of the relatively high dopant concentration (10% in this case) the formation of Co-O-Co is quite likely, as discussed below. Hence, at least 95% of the Co atoms are incorporated on Zn substitutional sites and the ZnO wurtzite lattice remains undisturbed by the dopant. This result convincingly shows that our films are of excellent structural quality, devoid of metallic Co, small Co clusters or antisite disorder within detection limits.

Figure 3(a) shows the normalized XANES and XMCD spectra recorded at the Co *K* edge at 6.7 K. A clear dichroic signal of the order of 0.3% with respect to the edge jump is visible at the preedge feature of Co, which signals the absence of metallic Co [2,4]. An element specific $M(H)$ curve was measured at the Co preedge feature [Fig. 3(b)].

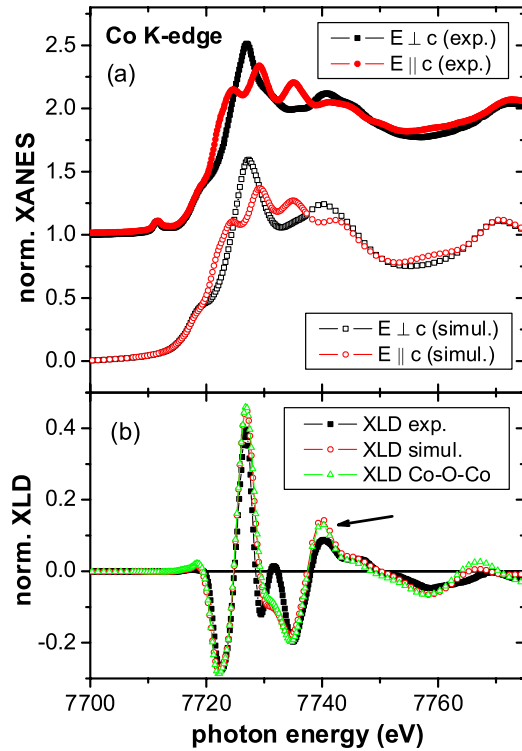


FIG. 2 (color online). (a) Measured and calculated XANES spectra at the Co K edge of Co:ZnO at 300 K and 10° grazing incidence. (b) Measured (full squares) and calculated XLD signatures of substitutional Co (open circles) and Co-O-Co pairs (open triangles).

To yield a more quantitative analysis we fit a Brillouin function to the $M(H)$ curves recorded at 6.7 and 40.5 K using $S = 3/2$ and $L = 3$ (yielding a magnetic moment μ for Co^{2+} of $6.63\mu_B$) as well as $S = 3/2$ and $L = 1.07$ (yielding a more typical Co^{2+} moment of $4.8\mu_B/\text{Co}^{2+}$ and the same value of $L/S = 0.7$ as in Ref. [4]). The only adjustment to the calculation was to normalize the value at saturation. The slightly better agreement between the fit with $L = 1.07$ and the experimental data is not significant; however, it indicates that the Co atoms have a magnetic moment of $(5 \pm 1)\mu_B$.

Figure 4 shows SQUID measurements for the same specimen as was used in Fig. 3. We did not detect any magnetic hysteresis at 300 K contrary to a previous study on sputtered Co:ZnO [4]. The diamagnetic background was derived from the high-field magnetization data at 300 K and subtracted from both data sets. At 5 K a clear paramagnetic signal can be seen after the same diamagnetic background is subtracted. As with the XMCD hysteresis, the SQUID data can be fitted well with the Brillouin function for $L = 1.07$, whereas the fit for $L = 3$ is not as good. From various fits of the SQUID loop (not shown) we conclude that the signal is caused by Co atoms with a moment $\mu = (4.8 \pm 0.4)\mu_B$, which compares well with the representative value for isolated Co^{2+} [12]. The inset shows field cooled versus zero field cooled curves; corroborating pure paramagnetism.

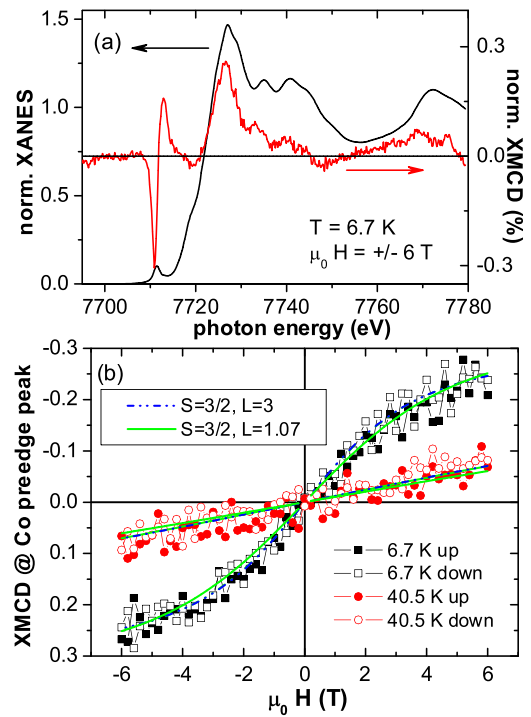


FIG. 3 (color online). (a) XANES and XMCD spectra recorded at the Co K edge at 6.7 K. (b) Two $M(H)$ curves recorded at the photon energy of the Co preedge XMCD feature at 6.7 K (squares) and at 40.5 K (circles) together with fitted Brillouin functions (see text).

So far we have derived the magnetic moment of the Co ions from the curvature of the $M(H)$ loop. By taking into account the sample volume and dopant concentration, we can calculate the expected overall magnetization for a magnetic moment of $(4.8 \pm 0.4)\mu_B$ [$\mu_z = (4.1 \pm 0.4)\mu_B$] per Co. This calculation yields a saturation magnetization of $(4.6 \pm 0.4) \times 10^{-4}$ emu which results in $(3.6 \pm 0.3) \times 10^{-4}$ emu after correcting for the SQUID measurement conditions (5 K and 5 T). In contrast, the SQUID measurements reveal only 1×10^{-4} emu which is only (28 ± 3) of the magnetization expected from the full moment, i.e., only $\mu = 1.4\mu_B$ ($\mu_z = 1.2\mu_B$) per Co effectively which would result in a linear $M(H)$ curve at 5 K in disagreement with both XMCD and SQUID results.

To explain this discrepancy, we consider the abundance of Co dopants on Zn substitutional sites in various clustered configurations using Behringer's equations for the hcp lattice [13]. For a Co mole fraction of $x = 0.1$, and assuming a random dopant distribution, the probabilities that a given Co dopant will have $n = 0, 1, 2$ other Co ions as next cation neighbors (i.e., isolated Co, Co-O-Co pairs, and triples) are given in the first two columns of Table I. With some approximations we also could estimate the abundance of Co quadruples ($n = 3$). Table I also shows four models assuming different effective magnetic moments per Co atom for the various configurations to calculate the effective fraction of the full moments. Here we

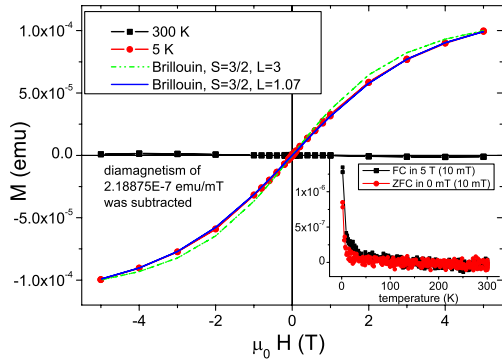


FIG. 4 (color online). SQUID $M(H)$ curves of Co:ZnO at 5 K and 300 K including fits using Brillouin functions for $L = 3$ (dashed line) and $L = 1.07$ (full line). Inset: Field cooled versus zero field cooled curves at 10 mT corroborating paramagnetic behavior.

restrict ourselves to collinear configurations of the moments. We consider Co in Co-O-Co configurations to be antiferromagnetically coupled as discussed recently [14]. Parallel alignment of the moments for pairs would yield $28.2 + 18.0 = 46.2\%$ of the full moment which is inconsistent with the SQUID data. All antiparallel triple configurations have an effective net moment of $1.6\mu_B$ per dopant (one up and two down, cases A and B). For the quadruples we also consider the partially compensated case (three up and one down) leading to $2.4\mu_B$ per atom effectively. However, since pairs are assumed to be compensated this should also hold for the quadruples, making case A and C unlikely. Obviously, the 28% reduction of the magnetization measured by SQUID can be readily explained by antiferromagnetic alignment for Co-O-Co pairs and negligible contributions to the moment from Co in triples (i.e., case D in Table I). Within the accuracy of the experiment only case B cannot be fully excluded. This could indicate that: (i) triples form less frequently as expected from a purely statistical model, or, (ii) that noncollinear configurations with an effective moment of about $1\mu_B$ have to be taken into account to be consistent with the reduced effective moment.

TABLE I. Apparent reduction of the full magnetic moment per dopant for the wurtzite structure.

No. of cation neighbors	Abundance	Case A	Case B	Case C	Case D
		μ_B/Co	μ_B/Co	μ_B/Co	μ_B/Co
$n = 0$ (single)	28.2%	4.8	4.8	4.8	4.8
$n = 1$ (pair)	18.0%	0	0	0	0
$n = 2$ (triple)	11.6%	1.6	1.6	0	0
$n = 3$ (quadruple)	$\approx 8\%$	2.4	0	2.4	0
Fraction of full moment		36.1%	32.1%	32.2%	28.2%

In conclusion, we have used XLD, XMCD, and SQUID to show that Co dopants in structurally excellent and compositionally well-defined $\text{Co}_{0.1}\text{Zn}_{0.9}\text{O}$ behave purely paramagnetically with a moment per isolated Co atom close to the well-established value of $4.8\mu_B$. The effective moment per Co is considerably less than $4.8\mu_B$ due to the formation of antiferromagnetic Co-O-Co type configurations which are in turn a natural consequence of a stochastic dopant distribution. Hence, we have no experimental evidence for intrinsic ferromagnetic interactions neither for isolated nor for paired Co dopants in high-quality Co:ZnO.

The work at the UDE was supported by the European Union under the Marie-Curie Excellence Grant No. MEXT-CT-2004-014195 of the 6th Framework Programme. The work at the Pacific Northwest National Laboratory was supported by the U.S. Department of Energy, Office of Science, Division of Materials Science and Engineering.

*ney@maglomat.de

- [1] P. Sati, R. Hayn, R. Kuzian, S. Régnier, S. Schäfer, A. Stepanov, C. Morhain, C. Deparis, M. Laügt, M. Goiran, and Z. Golacki, Phys. Rev. Lett. **96**, 017203 (2006).
- [2] K. R. Kittilstved, D. A. Schwartz, A. C. Tuan, S. M. Heald, S. A. Chambers, and D. R. Gamelin, Phys. Rev. Lett. **97**, 037203 (2006).
- [3] M. Venkatesan, P. Stamenov, L. S. Dorneles, R. D. Gunning, B. Bernoux, and J. M. D. Coey, Appl. Phys. Lett. **90**, 242508 (2007).
- [4] A. Barla, G. Schmerber, E. Beaurepaire, A. Dinia, H. Bieber, S. Colis, F. Scheurer, J.-P. Kappler, P. Imperia, F. Nolting, F. Wilhelm, A. Rogalev, D. Müller, and J. J. Grob, Phys. Rev. B **76**, 125201 (2007).
- [5] E. Sarigiannidou, F. Wilhelm, E. Monroy, R. M. Galera, E. Bellet-Amalric, A. Rogalev, J. Goulon, J. Cibert, and H. Mariette, Phys. Rev. B **74**, 041306(R) (2006).
- [6] A. Ney, T. Kammermeier, E. Manuel, V. Ney, S. Dhar, K. H. Ploog, F. Wilhelm, and A. Rogalev, Appl. Phys. Lett. **90**, 252515 (2007).
- [7] T. C. Kaspar, S. M. Heald, C. M. Wang, J. D. Bryan, T. Droubay, V. Shutthanandan, S. Thevuthasan, D. E. McCready, A. J. Kellock, D. R. Gamelin, and S. A. Chambers, Phys. Rev. Lett. **95**, 217203 (2005).
- [8] A. Rogalev, J. Goulon, C. Goulon-Ginet, and C. Malgrange, Lect. Notes Phys. **565**, 61 (2001).
- [9] Y. Joly, Phys. Rev. B **63**, 125120 (2001).
- [10] E. H. Kisi and M. M. Elcombe, Acta Crystallogr. Sect. C **45**, 1867 (1989).
- [11] M. O. Krause and J. H. Oliver, J. Phys. Chem. Ref. Data **8**, 329 (1979).
- [12] C. Kittel, *Einführung in die Festkörperphysik* (Oldenbourg, München, Wien, 1999).
- [13] R. E. Behringer, J. Chem. Phys. **29**, 537 (1958).
- [14] T. Dietl, T. Andrearczyk, A. Lipinska, M. Kiecana, M. Tay, and Y. Wu, Phys. Rev. B **76**, 155312 (2007).